HOKKAIDO UNIVERSITY

Title	Feasibility study of decay heat uncertainty reduction using nuclear data adjustment method with experimental data
Author(s)	Kawamoto, Yosuke; Chiba, Go
Citation	Journal of nuclear science and technology, 54(2), 213-222 https://doi.org/10.1080/00223131.2016.1238785
Issue Date	2017-02
Doc URL	https://hdl.handle.net/2115/68242
Rights	This is an Accepted Manuscript of an article published by Taylor & Francis in Journal of nuclear science and technology on Feb 2017, available online: http://www.tandfonline.com/10.1080/00223131.2016.1238785.
Type	journal article
File Information	report_kawamoto.pdf



Hokkaido University Collection of Scholarly and Academic Papers : HUSCAP

ARTICLE

Typeset with jnst.cls <ver.1.84>

Feasibility study of decay heat uncertainty reduction using nuclear data adjustment method with experimental data

Yosuke Kawamoto and Go Chiba*

Nuclear Reactor Engineering Laboratory, Division of Energy and Environmental Systems, Graduate School of Engineering, Hokkaido University, Sapporo, Hokkaido 060-8628, Japan

The accurate prediction of the decay heat is essential, especially for nuclear power plant safety purposes. However, it is known that the decay heat predicted by nuclear fuel burnup calculations is uncertain because of uncertainty of nuclear data employed in the calculations.

If the decay heat uncertainty can be reduced, the safety margin of the predicted decay heat can also be reduced, and feasible design ranges of various types of equipments related to the decay heat can be extended. In the present study, we use the nuclear data adjustment method for the decay heat uncertainty reduction with several types of the experimental data. As a result, we clarify that the decay heat uncertainty with short and long-term cooling periods can be reduced by this method with appropriate experimental data.

Keywords: nuclear data adjustment method, decay heat uncertainty, post irradiation examination data, fission pulse decay heat data, generalized perturbation theory

*Corresponding author. Email: go_chiba@eng.hokudai.ac.jp

1. Introduction

The accurate prediction of the decay heat is essential, especially for nuclear power plant safety purposes, and the decay heat is predicted by nuclear fuel burn-up calculations. In the burn-up calculations, isotopic concentrations are calculated with time, and then the decay heat is evaluated from the isotopic concentrations at an arbitrary time. During the calculations, neutron transport and fuel depletion calculations are done alternately, and various nuclear data, such as neutron reaction cross sections, fission yields and decay constants of each nuclide, are used. Thus the accuracy of the predicted decay heat depends on the employed nuclear data largely. Actually, it is known that there is non-negligible nuclear data induced uncertainty in decay heat predicted by the burn-up calculations[1,2], so the design values of decay heat, which are used for engineering purposes, should include safety margin generally. If such a decay heat uncertainty can be reduced, the safety margin can also be reduced, and feasible design ranges of various types of equipments related to the decay heat can be extended.

One of the major methods to reduce the nuclear data induced uncertainty is the nuclear data adjustment method[3]. This method has been mainly used for uncertainty reduction of neutronics parameters of fast neutron reactors. In this method, nuclear data are adjusted within a range of their own uncertainties to match calculation results with experimental data on integral quantities of nuclear reactors. With this process, the uncertainty of nuclear data can be reduced, so prediction of parameters which depend on the nuclear data can be performed with reduced uncertainty. In the present study, we apply the nuclear data adjustment method to the decay heat uncertainty reduction. We consider not only neutron reaction cross sections but also fission yields, decay constants and so on as the nuclear data to be adjusted. We employ fission pulse decay heat data and Post Irradiation Examination (PIE) data of nuclear fuel composition for the adjustment. If this method works well, we can reduce the decay heat uncertainty using the experi-

mental data. Since the decay heat measurement of the actual nuclear fuel is not easy, the proposed approach is considered effective.

In the present study, first, we perform uncertainty propagation calculation from the nuclear data to the decay heat of spent nuclear fuels with short and long-term cooling periods, which are "target" decay heat whose uncertainties are attempted to be reduced. In this uncertainty propagation process, sensitivity coefficients of the decay heat with respect to the nuclear data are necessary, and these are calculated by a numerical procedure based on the generalized perturbation theory. Secondly, we perform the uncertainty propagation calculation from the nuclear data to the experimental data used for the nuclear data adjustment. Moreover, we calculate the correlation between the target decay heat and experimental data uncertainties. It is known that the stronger this correlation is, the more the uncertainty can be reduced with the nuclear data adjustment method. We can specify the effective experimental data for the adjustment method from this correlation information. Finally, we perform the nuclear data adjustment to reduce the uncertainty of the target decay heat using the experimental data.

2. Theory

In this section, we describe the theories of the generalized perturbation theory(GPT)-based burn-up sensitivity calculation in Subsection 2.1, the uncertainty propagation calculation in Subsection 2.2 and the nuclear data adjustment method in Subsection 2.3.

2.1 GPT-based burn-up sensitivity calculation

We consider a parameter R depending on a nuclear data σ. We define a relative sensitivity coefficient of R to σ, S_σ^R, as

$$S_\sigma^R = \frac{\partial R}{\partial \sigma} \cdot \frac{\sigma}{R}. \tag{1}$$

This sensitivity is numerically calculated with GPT[4]. In this subsection, we briefly explain the theory of the burn-up sensitivity calculation based on GPT.

Let us calculate a sensitivity of nuclide number densities to a nuclear data σ. The burn-up equation can be written as

$$\frac{d\mathbf{n}(t)}{dt} = \mathbf{A}\mathbf{n}(t), \tag{2}$$

where $\mathbf{n}(t)$ is a nuclide number density vector at t and $\mathbf{A}$ is a burn-up matrix. The vector $\mathbf{n}(t)$ can be written as the following equation which is the analytic solution of Eq.(2);

$$\mathbf{n}\left(t\right) = \exp\left(\mathbf{A}t\right)\mathbf{n}\left(0\right). \tag{3}$$

If σ is perturbed as $\sigma + \Delta\sigma$, the burn-up equation for the perturbed system can be written as

$$\frac{d\left(\mathbf{n} + \Delta\mathbf{n}\right)}{dt} = \left(\mathbf{A} + \Delta\mathbf{A}\right)\left(\mathbf{n} + \Delta\mathbf{n}\right), \tag{4}$$

where time dependence of $\mathbf{n}$ and $\Delta\mathbf{n}$ are omitted here. If we assume the term $\Delta\mathbf{A}\Delta\mathbf{n}$ is negligible, the difference between Eq.(4) and Eq.(2) is

$$\frac{d\Delta\mathbf{n}}{dt} = \Delta\mathbf{A}\mathbf{n} + \mathbf{A}\Delta\mathbf{n}. \tag{5}$$

The both sides of Eq.(5) are multiplied by a time-dependent weight function $\mathbf{w}(t)$;

$$\mathbf{w}^{\mathrm{T}}\frac{d\Delta\mathbf{n}}{dt} = \mathbf{w}^{\mathrm{T}}\Delta\mathbf{A}\mathbf{n} + \mathbf{w}^{\mathrm{T}}\mathbf{A}\Delta\mathbf{n}, \tag{6}$$

where the superscript T means transpose of a matrix or a vector. Time dependence of $\mathbf{w}$ is also omitted here. Suppose that the considering period is from 0 to P seconds. We integrate the both sides of Eq.(6) over this time period as

$$\int_0^{\mathrm{P}} \mathbf{w}^{\mathrm{T}}\frac{d\Delta\mathbf{n}}{dt}dt = \int_0^{\mathrm{P}} \mathbf{w}^{\mathrm{T}}\Delta\mathbf{A}\mathbf{n}dt + \int_0^{\mathrm{P}} \mathbf{w}^{\mathrm{T}}\mathbf{A}\Delta\mathbf{n}dt. \tag{7}$$

We define the function $\mathbf{w}(t)$ as

$$\mathbf{A}^{\mathrm{T}}\mathbf{w}(t) = -\frac{d\mathbf{w}\left(t\right)}{dt}. \tag{8}$$

The function $\mathbf{w}(t)$ is called *adjoint number density* and is written as the following equation

which is the analytic solution of Eq.(8);

$$\mathbf{w}\left(t\right)=\exp\left(\mathbf{A}^{\mathrm{T}}\left(P-t\right)\right)\mathbf{w}\left(P\right). \tag{9}$$

During the period [0,P], Eq.(9) is calculated from the end of the period to the beginning as if it goes back in time.

Using Eq.(8), the second term of the right hand side of Eq.(7) can be written as

$$\int_0^{\mathrm{P}}\mathbf{w}^{\mathrm{T}}\mathbf{A}\Delta\mathbf{n}dt=\int_0^{\mathrm{P}}\Delta\mathbf{n}^{\mathrm{T}}\mathbf{A}^{\mathrm{T}}\mathbf{w}dt=-\int_0^{\mathrm{P}}\Delta\mathbf{n}^{\mathrm{T}}\frac{d\mathbf{w}\left(t\right)}{dt}dt, \tag{10}$$

and then Eq. (7) can be rewritten as

$$\begin{aligned}
\int_0^{\mathrm{P}}\mathbf{w}^{\mathrm{T}}\frac{d\Delta\mathbf{n}}{dt}dt &= \int_0^{\mathrm{P}}\mathbf{w}^{\mathrm{T}}\Delta\mathbf{A}\mathbf{n}dt-\int_0^{\mathrm{P}}\Delta\mathbf{n}^{\mathrm{T}}\frac{d\mathbf{w}\left(t\right)}{dt}dt,\\
\int_0^{\mathrm{P}}\mathbf{w}^{\mathrm{T}}\frac{d\Delta\mathbf{n}}{dt}dt+\int_0^{\mathrm{P}}\Delta\mathbf{n}^{\mathrm{T}}\frac{d\mathbf{w}\left(t\right)}{dt}dt &= \int_0^{\mathrm{P}}\mathbf{w}^{\mathrm{T}}\Delta\mathbf{A}\mathbf{n}dt,\\
\int_0^{\mathrm{P}}\frac{d}{dt}\left(\mathbf{w}^{\mathrm{T}}\Delta\mathbf{n}\right)dt &= \int_0^{\mathrm{P}}\mathbf{w}^{\mathrm{T}}\Delta\mathbf{A}\mathbf{n}dt,\\
\mathbf{w}\left(\mathrm{P}\right)^{\mathrm{T}}\Delta\mathbf{n}\left(\mathrm{P}\right)-\mathbf{w}\left(0\right)^{\mathrm{T}}\Delta\mathbf{n}\left(0\right) &= \int_0^{\mathrm{P}}\mathbf{w}^{\mathrm{T}}\Delta\mathbf{A}\mathbf{n}dt,\\
\mathbf{w}\left(\mathrm{P}\right)^{\mathrm{T}}\Delta\mathbf{n}\left(\mathrm{P}\right) &= \int_0^{\mathrm{P}}\mathbf{w}^{\mathrm{T}}\Delta\mathbf{A}\mathbf{n}dt\ \left(\because\Delta\mathbf{n}\left(0\right)=0\right).
\end{aligned} \tag{11}$$

We define that $\mathbf{w}\left(P\right)$ is $\mathbf{e}_i$, where the element which corresponds to the nuclide i is unity and all other elements are zero. With this final condition, Eq.(11) is transformed as

$$\Delta n_i\left(\mathrm{P}\right)=\int_0^{\mathrm{P}}\mathbf{w}^{\mathrm{T}}\Delta\mathbf{A}\mathbf{n}dt, \tag{12}$$

where n_i is the number density of the nuclide i, and a sensitivity of n_i to σ can be written as

$$\frac{dn_i}{d\sigma}\approx\frac{\Delta n_i}{\Delta\sigma}=\frac{\int_0^{\mathrm{P}}\mathbf{w}^{\mathrm{T}}\Delta\mathbf{A}\mathbf{n}dt}{\Delta\sigma}. \tag{13}$$

In the burn-up sensitivity calculations, the forward nuclide number density is calculated first, and then the adjoint number density is calculated starting with the final adjoint number density $\mathbf{e}_i$ at the end of the considering period with direction going back in time. Once the forward and adjoint number densities are obtained, the sensitivity of the number density to any nuclear data can be calculated with Eq.(13).

The decay heat H is calculated as

$$H = \sum_i \left(E_i \lambda_i n_i \right), \tag{14}$$

where E_i is total decay energy per a decay and λ_i is the decay constant of the nuclide i. In the case of decay heat sensitivity calculations, we should consider both the direct effect through the decay constant or decay energy change and the indirect effect through the number density change to the decay heat. The sensitivity of H to E_j is written as

$$S^H_{E_j} = \frac{dH}{dE_j} \cdot \frac{E_j}{H} = \frac{E_j \lambda_j n_j}{H}. \tag{15}$$

According to Eq.(15), it suffices to consider only the direct effect for the sensitivity to the decay energy because $\mathbf{n}$ does not depend on the decay energy. On the other hand, the indirect effect should be taken into account when one calculates sensitivity of H to λ because $\mathbf{n}$ depends on λ. The sensitivity of H to λ_j is written as

$$S^H_{\lambda_j} = \frac{dH}{d\lambda_j} \cdot \frac{\lambda_j}{H} = \frac{E_j \lambda_j n_j}{H} + \sum_k \left(\frac{\partial H}{\partial n_k} \cdot \frac{\partial n_k}{\partial \lambda_j} \right) \cdot \frac{\lambda_j}{H} = \frac{E_j \lambda_j n_j}{H} + \left\{ \sum_k \left(E_k \lambda_k \right) \frac{\partial n_k}{\partial \lambda_j} \right\} \frac{\lambda_j}{H}. \tag{16}$$

The second term on the right hand side of Eq.(16) is called the indirect sensitivity term which is calculated by using GPT. In such a case, the final condition of adjoint number density is not $\mathbf{e}_i$, but the product of the decay constant and the decay energy for every nuclides.

Although sensitivity to the decay branching ratio can be calculated similarly, the sensitivity coefficient should be corrected so that the summation of the branching ratio is unity. In order to consider this normalization condition, we use the following equation[5];

$$\overline{S^H_{b_{i,j}}} = S^H_{b_{i,j}} - b_{i,j} \sum_{k=1}^{B_i} S^H_{b_{i,k}}, \tag{17}$$

where $\overline{S}$ is the corrected sensitivity coefficient considering the normalization condition, $b_{i,j}$ is the jth branching ratio of the nuclide i and B_i is the total number of branching channels of the nuclide i.

In the above mentioned burn-up sensitivity, we consider only the effect of the burn-up

matrix element change caused by perturbation in nuclear data to the isotopic generation or the decay heat. However, since neutron transport calculation is also performed in spatially-dependent burn-up calculations, we should also consider the effect through neutron flux change caused by the nuclear data perturbation. Thus, in our calculations, the generalized adjoint neutron flux and the adjoint power are also calculated, and the obtained sensitivity coefficients include all these perturbation effects. The detail of the method how to calculate the sensitivity coefficients using the generalized adjoint neutron flux and the adjoint power is explained in our previous paper[6]. For the fission pulse decay heat cases, we can apply Eqs.(13), (15) and (16) to the sensitivity calculations since we do not have to consider the spatial dependence in such cases.

2.2 Uncertainty propagation calculation

The uncertainty propagation calculation is carried out as

$$v = \mathbf{g}^{\mathrm{T}}\mathbf{M}\mathbf{g}, \tag{18}$$

where v is the variance of a parameter (e.g. decay heat), $\mathbf{g}$ is a vector which contains sensitivity coefficients of the parameter to the nuclear data, and $\mathbf{M}$ is a covariance matrix of the nuclear data. In the case of the plural parameters, a covariance matrix of the parameters $\mathbf{V}$ is obtained as

$$\mathbf{V} = \mathbf{G}^{\mathrm{T}}\mathbf{M}\mathbf{G}, \tag{19}$$

where $\mathbf{G}$ is a matrix which contains the plural $\mathbf{g}$ corresponding to each parameter in the form of vector. In this case, we can also calculate the correlation between the different parameter uncertainties as shown in Subsection 5.3.

We quantify the decay heat uncertainty and correlation using these equations with the sensitivity coefficients and the covariance data of the nuclear data.

2.3 Nuclear data adjustment method

The nuclear data adjustment is the method based on the Bayesian approach which adjusts nuclear data to maximize the probability of the nuclear data being true values under a condition that additional experimental data are obtained. According to Ref.[3], the basic equations of the nuclear data adjustment method are described as follows. First, a relative change in nuclear data through the adjustment is written as

$$\mathbf{D}_{xs} = \mathbf{MG}\left(\mathbf{G}^{\mathrm{T}}\mathbf{MG} + \mathbf{V_e} + \mathbf{V_m}\right)^{-1}\mathbf{D}_{c/e-1}, \tag{20}$$

where $\mathbf{D}_{xs}$ is a vector containing relative change of the nuclear data, $\mathbf{V_e}$ and $\mathbf{V_m}$ are covariance matrices of the experimental and calculation uncertainties, respectively, and $\mathbf{D}_{c/e-1}$ is a vector containing relative differences between the calculation and experimental values $(C/E-1)$. The nuclear data uncertainty can be reduced by the adjustment, and the posterior covariance matrix of nuclear data $\mathbf{M}'$ is written as

$$\mathbf{M}' = \mathbf{M} - \mathbf{MG}\left(\mathbf{G}^{\mathrm{T}}\mathbf{MG} + \mathbf{V_e} + \mathbf{V_m}\right)^{-1}\mathbf{G}^{\mathrm{T}}\mathbf{M}. \tag{21}$$

The effect of the nuclear data adjustment to parameters which are not used in the adjustment procedure can be calculated by multiplying the nuclear data change and the sensitivity coefficients as

$$\mathbf{D}_{para} = \mathbf{G}_{para}^{\mathrm{T}}\mathbf{D}_{xs} = \mathbf{G}_{para}^{\mathrm{T}}\mathbf{MG}\left(\mathbf{G}^{\mathrm{T}}\mathbf{MG} + \mathbf{V_e} + \mathbf{V_m}\right)^{-1}\mathbf{D}_{c/e-1},$$

where $\mathbf{D}_{para}$ is a vector containing relative changes of the parameters and $\mathbf{G}_{para}$ is a matrix containing sensitivity coefficients of the parameters to the nuclear data. A covariance matrix of the parameters $\mathbf{V}_{para}$ is written as

$$\begin{aligned}\mathbf{V}_{para} &= \mathbf{G}_{para}^{\mathrm{T}}\mathbf{M}'\mathbf{G}_{para} \\ &= \mathbf{G}_{para}^{\mathrm{T}}\mathbf{MG}_{para} - \mathbf{G}_{para}^{\mathrm{T}}\mathbf{MG}\left(\mathbf{G}^{\mathrm{T}}\mathbf{MG} + \mathbf{V_e} + \mathbf{V_m}\right)^{-1}\mathbf{G}^{\mathrm{T}}\mathbf{MG}_{para}.\end{aligned} \tag{22}$$

In the case of burn-up calculation, we should consider not only the cross section but also the fission yield, the decay constant (or the half life), the decay energy and the decay

branching ratio.

According to Eqs.(20) and (21), covariance data of the experimental data and calculation results should be quantified in order to perform the adjustment. Since the uncertainty of the experimental data is given redonly as a standard deviation in many cases, the correlation between the experimental data uncertainties should be assumed in some ways. Concerning the uncertainty of the calculation values, it is quite difficult to quantify it when one employs deterministic code systems. Since we use a deterministic code system in the present study, we employ sufficiently conservative values for the uncertainty.

3. Problem specification

In the present study, we perform burn-up uncertainty calculations for the target decay heat whose uncertainties are attempted to be reduced, and for the several experimental data which are used in the adjustment procedure. These specifications are described in this section.

3.1 Target decay heat

As the target decay heat, we perform pin-cell burn-up calculations of a 3.8% enriched UO_2 fuel with burn-up of 20 GWd/t and two different cooling periods: short-term (10^{-1}∼10^5 [s]) and long-term (10^{-1}∼10^3 [yr]). The irradiation power density is constant at 179[W/cm]; a complicated power history is not considered. Actually geometrical specification, material composition and other physical conditions of this UO_2 cell is the same as that of a UO_2 fuel of the PIE data used for the adjustment.

3.2 Experimental data used for the nuclear data adjustment

For the nuclear data adjustment, we employ the two types of experimental data: the fission pulse decay heat data and the PIE isotopic concentration data. The employed

experimental data in the present study are summarized in **Table 1**.

The fission pulse decay heat data are uranium-235 and plutonium-239 with the thermal neutron irradiation (LOWELL[7]), uranium-235, plutonium-239 and -241 with the thermal neutron irradiation (ORNL[8–10]) and uranium-238 with the fast neutron irradiation (YAYOI[11, 12]).

The PIE data are the UO_2 and MOX fuels[13, 14]. Uranium enrichment of the UO_2 fuel is 3.8% and the plutonium enrichment of the MOX fuel is 5.07 wt%. The detailed informations such as geometrical specification, material composition and burnup conditions are provided in Refs.[13, 14]. Conditions which are not described in these references are decided as general values from Refs.[15, 16].

Concerning the uncertainty of the experimental data, we employ the standard deviations given in Refs.[7–14]. Unfortunately correlations between experimental data are not provided in any references even though strong positive correlations are expected among measurement data at different cooling time in the same series of decay heat measurements. We assume that the correlation between experimental data uncertainties is zero for the PIE data and 0.8 for the fission pulse data. This assumption of the correlation in the fission pulse data is discussed in a different paper written by one of the present authors[17], and it is shown in this paper that the strong correlation of 0.8 is not a bad assumption.

[Table 1 about here.]

4. Calculation methods and covariance data of nuclear data

In this section, we describe the burn-up calculation methods and covariance data of nuclear data which are used in the uncertainty propagation and nuclear data adjustment calculations.

4.1 Burn-up calculation methods

In the present study, all the calculations are done by CBZ, a multi-purpose reactor physics calculation code system which is under development at Hokkaido University.

In the pin-cell burn-up calculations, resonance self-shielding, neutron transport and depletion calculations are done alternately during the whole cycle. The self-shielding calculation is based on the equivalence theory with the advanced Bondarenko model[18]. The neutron transport calculation is done with the collision probability method for a two-dimensional square pin-cell model. 107-group cross section is used for the transport calculations. The depletion calculation is done by the matrix exponential method with the MMPA method[19]. The burn-up chain which we use includes 21 actinide nuclides and 1284 fission product (FP) nuclides, which are all the nuclides provided in JENDL/FPD-2011[20]. We use JENDL-4.0[21] for the neutron reaction cross sections. Concerning europium-156, we use the updated one (JENDL-4.0u). JENDL/FPY-2011[20] and FPD-2011 are used for the fission yields and the decay data.

In the fission pulse decay heat calculations, only the depletion calculations are done. In these calculations, the initial nuclide composition is the independent fission yields of the considering fissionable nuclide. The depletion calculation method is the same as the pin-cell burn-up calculation.

We assume that the calculation uncertainty is 2% for the nuclide number densities which are evaluated by the pin-cell burn-up calculations and 0.01% for the decay heat which are evaluated by the fission pulse decay heat calculations. No correlations between these calculation result uncertainties are considered.

4.2 Covariance data of nuclear data

For the uncertainty propagation and nuclear data adjustment calculations, we employ the covariance data of nuclear data given in the evaluated nuclear data files. The origin

of the uncertainty data are summarized in **Table 2**.

On the neutron reaction cross sections, we employ the covariance data of the actinide nuclides from JENDL-4.0. Since there is no covariance data of the FP nuclides in JENDL-4.0, we employ the data from TENDL-2014[22]. On the other nuclear data such as fission yields and decay constants of FP nuclides, we employ the uncertainty information given in JENDL/FPD-2011 and JENDL/FPY-2011. The uncertainty of the actinide decay data is not given in JENDL/FPD-2011. According to Ref.[23], the uncertainty of the actinide decay data is negligible for the decay heat uncertainty, so we do not consider it.

For the fission yields and decay data, the uncertainty data are given in the nuclear data libraries as standard deviations, not covariance data. We assume that there are no correlations for the half life, the decay energy and the decay branching ratio. However, for the fission yield, it is known that one should consider the correlation between the FP nuclide uncertainties which belong to the same decay path[1]. Thus, we use the equation which is based on the Bayesian approach in order to calculate the correlation between the FP nuclide uncertainties, which is described in Ref.[1]. For some short half-lived nuclides, the standard deviations of their decay data are not provided in the libraries, so the uncertainties of these data are assumed 100%.

[Table 2 about here.]

5. Numerical Results

In this section, numerical results of nuclear data induced uncertainties of the target decay heat and the experimental data, the correlation between them, and the uncertainty reduction of the target decay heat are shown.

5.1 Target decay heat uncertainty

The target decay heat uncertainty curves of the UO_2 fuel with contributions of each nuclear data uncertainty for the short and long-term cooling periods are shown in **Figures 1** and **2**, respectively.

According to Figure 1, the dominant component of the short-term decay heat uncertainty is the decay energy uncertainty. The contribution of the fission yield uncertainty is around 0.4%, and those of the cross section, half life and branching ratio uncertainties are negligible. The total uncertainty is around 3% from 0.1 to 100 [s], then decreases with time, and becomes less than 1% after 1000 [s]. The dominant components of the uncertainty from 0.1 to 100 [s] are the decay energy uncertainties of various nuclides which are assumed 100%.

According to Figure 2, the dominant components of the long-term decay heat uncertainty are the decay energy and cross section uncertainties. The contribution of the fission yield uncertainty is around 0.4%, and those of the half life and branching ratio uncertainties are negligible. There is an uncertainty peak ($\sim$ 3%) at 10 [yr], and the cause of this peak is the beta decay energy uncertainty of barium-137m which is assumed 100%. Barium-137m is a daughter nuclide of cesium-137, and the γ component of its decay energy is much larger than the β component; the former is 59.48 keV and the latter is 6.36 keV redaccording to JENDL/FPD-2011. In this library, uncertainty of 1.0 keV is given to the γ component whereas no uncertainty information is provided in the β component. There is also an uncertainty peak ($\sim$ 2.3%) at 300 [yr], and the cause of this peak is the capture cross section uncertainties of the several actinide nuclides, such as uranium-238, plutonium-239, -240 and -241.

[Figure 1 about here.]

[Figure 2 about here.]

5.2 C/E ratios and nuclear data induced uncertainty of experimental data

Figure 3 shows C/E-1 values of the fission pulse decay heat data of uranium-235 with the thermal neutron irradiation (LOWELL and ORNL) with error bars of the measurement (1σ) and the nuclear data induced uncertainty. Other than this, various fission pulse decay heat data are also used for the adjustment calculations as mentioned in Subsection 3.2, but numerical results of these data are omitted here.

Figures 4 and **5** show C/E-1 values of the PIE data with error bars of the measurement and nuclear data induced uncertainty of the UO_2 and MOX fuels, respectively.

These C/E values are used in the following nuclear data adjustment calculations.

[Figure 3 about here.]

[Figure 4 about here.]

[Figure 5 about here.]

5.3 Correlation between target decay heat and experimental data

Correlation matrices between the short-term target decay heat uncertainty and the fission pulse decay heat uncertainty of the uranium-235 with the thermal neutron irradiation are shown in **Figure 6**. Matrices between the long-term target decay heat uncertainty and the fission pulse decay heat uncertainty are shown in **Figure 7**. Figure 6 shows strong positive correlations over the whole cooling period, so we can expect that the nuclear data adjustment using the fission pulse experimental data can reduce the short-term decay heat uncertainty efficiently. In contrast to the short-term decay heat case, Figure 7 shows no correlation over the whole cooling period. Thus, we can expect that the nuclear data adjustment using the fission pulse experimental data cannot reduce the long-term decay heat uncertainty. The tendency of these results is the same as the results with the uranium-238, plutonium-239 and -241 fission pulse decay heat data.

Correlation matrices between the short-term target decay heat uncertainty and the

PIE isotopic concentration data uncertainty are shown in **Figure 8**. Matrices between the long-term target decay heat uncertainty and the PIE data uncertainty are shown in **Figure 9**. Figure 8 shows weak positive correlations between the target uncertainty and the isotopic generation uncertainties of several nuclides. Thus, we can expect that the impact of the nuclear data adjustment using the PIE data on the short-term decay heat uncertainty is restrictive or little. On the other hand, Figure 9 shows strong positive or negative correlations between the target uncertainty and the isotopic generation uncertainties of several nuclides. Thus, we can expect that the nuclear data adjustment using the PIE data can reduce the long-term decay heat uncertainty efficiently.

[Figure 6 about here.]

[Figure 7 about here.]

[Figure 8 about here.]

[Figure 9 about here.]

5.4 Reduction of target decay heat uncertainty

The short and long-term target decay heat uncertainty curves before and after the nuclear data adjustment using the fission pulse decay heat data are shown in **Figure 10**. Although the long-term decay heat uncertainty does not change by the adjustment completely, the short-term one is reduced by the fission pulse data efficiently. These results are consistent with the expectation from the correlation matrices in Subsection 5.3. It is considered that the dominant component of the reduced uncertainty is the decay energy uncertainties of the short half-lived nuclides which are assumed 100%. In other words, the adjustment with the fission pulse data can revise the assumed decay energy uncertainties of the short half-lived nuclides. Since the fission pulse data reflect the decay data of the short half-lived nuclides mainly, these are efficient in the short-term decay heat uncertainty reduction.

The short and long-term target decay heat uncertainty curves before and after the nuclear data adjustment using the PIE isotopic concentration data are shown in **Figure 11**. The long-term decay heat uncertainty is reduced by the PIE data, and the short-term one is slightly reduced by the adjustment. This result is also consistent with the expectation in Subsection 5.3. The uncertainty peak at 300 [yr] in Figure 11(b) is reduced by around half, but the peak at 10 [yr] is not. The former peak is caused by the actinide cross section uncertainties, and it can be reduced by the adjustment with the PIE data. However, the latter peak is caused by the barium-137m decay energy uncertainty, and it cannot be reduced by the adjustment. Thus, if the barium-137m decay energy uncertainty can be reduced from 100%, we can reduce the long-term decay heat uncertainty around 10 [yr] after the reactor shutdown.

[Figure 10 about here.]

[Figure 11 about here.]

6. Conclusion

We have performed the uncertainty propagation calculations of the decay heat, and have quantified the component-wise uncertainty of the target UO_2 fuel with the short and long-term cooling periods. The JENDL nuclear data libraries have been used and the maximum uncertainties of both cases are around 3%. The dominant components of the uncertainty are the decay energy uncertainty for the short-term decay heat, and the decay energy and cross section uncertainties for the long-term decay heat. Additionally, we have calculated the correlation between the target decay heat and experimental data uncertainties, and have considered the effectiveness of the nuclear data adjustment method using the experimental data in the uncertainty reduction of the target decay heat. It has been expected that the fission pulse decay heat data are effective for the uncertainty reduction of the short-term decay heat, and the PIE data are for the long-term one.

We have applied the nuclear data adjustment method to the decay heat uncertainty reduction using various experimental data. As a result, the short-term target decay heat uncertainty can be reduced effectively by the fission pulse decay heat data, and long-term one can be reduced partially by the PIE data. These results are consistent with the expectations from the correlation information.

We have proved that the decay heat uncertainty can be reduced by the nuclear data adjustment method using appropriate experimental data. There exist several experimental data of long-term decay heat of spent fuels discharged from actual power reactors. Addition of such other experimental data enables us to further reduce the prediction uncertainty of the long-term decay heat.

References

[1] Katakura J. Uncertainty analyses of decay heat summation calculations using JENDL, JEFF, and ENDF files. J Nucl Sci Technol. 2013;50:799-807.

[2] Rochman D, Koning AJ, Da Cruz DF. Propagation of ^{235,236,238}U and ^{239}Pu nuclear data uncertainties for a typical PWR fuel element. Nucl Technol. 2010;179:323-338.

[3] Dragt JB, Dekker JWM, Gruppelaar H, Janssen AJ. Method of adjustment and error evaluation of neutron capture cross sections; application to fission product nuclides. Nucl Sci Eng. 1977;62:117-129.

[4] Williams ML, Development of depletion perturbation theory for coupled neutron/nuclide fields. Nucl Sci Eng. 1979;70:20-36.

[5] Chiba G, Tsuji M, Narabayashi T. Sensitivity analysis for reactor stable period induced by positive reactivity using one-point adjoint kinetic equation. J Nucl Sci Technol. 2013;50:1150-1160.

[6] Chiba G, Kawamoto Y, Narabayashi T. Development of fuel depletion sensitivity calculation module for multi-cell problems in deterministic reactor physics code system CBZ. Ann Nucl Energy. 2016;96;313-323.

[7] Seabury EH, Li S, Nguyen HV, Campbell JM, Couchell GP, Pullen DJ, Schier WA, Tipnis SV.

Decay heat measurements following neutron fission of ^{235}U and ^{239}Pu. Proceedings of International Conference on Nuclear Data for Science and Technology; 1997; Trieste, Italy.

[8] Dickens JK, Emery JF, Love TA, McConnell JW, Northcutt KJ, Peelle RW, Weaver H. Fission product energy release for time following thermal neutron fission of ^{235}U between 2 and 14,000 seconds. Oak Ridge (Tennessee):Oak Ridge National Laboratory;1977.

[9] Dickens JK, Emery JF, Love TA, McConnell JW, Northcutt KJ, Peelle RW, Weaver H. Fission product energy release for time following thermal neutron fission of ^{239}Pu between 2 and 14,000 seconds. Oak Ridge (Tennessee):Oak Ridge National Laboratory;1977.

[10] Dickens JK, Emery JF, Love TA, McConnell JW, Northcutt KJ, Peelle RW, Weaver H. Fission product energy release for time following thermal neutron fission of ^{241}Pu between 2 and 14,000 seconds. Oak Ridge (Tennessee):Oak Ridge National Laboratory;1978.

[11] Akiyama M, Furuta K, Ida T, Sakata K, An S. Measurements of beta-ray decay heat of fission products for fast neutron fission of ^{235}U, ^{239}Pu and ^{233}U. J At Energy Soc Jpn. 1982;24:803-816. [in Japanese]

[12] Akiyama M, Furuta K, Ida T, Sakata K, An S. Measurements of gamma-ray decay heat of fission products for fast neutron fission of ^{235}U, ^{239}Pu and ^{233}U. J At Energy Soc Jpn. 1982;24:709-722. [in Japanese]

[13] Sasahara A, Matsumura T, Nicolaou G, Kiyanagi Y. Isotopic analysis of actinides and fission products in LWR high-burnup UO_2 spent fuels and its comparison with nuclide composition calculated using JENDL, ENDF/B, JEF and JEFF. J Nucl Sci Technol. 2008;45:313-327.

[14] Sasahara A, Matsumura T, Nicolaou G, Kiyanagi Y. Chemical isotopic analysis of fission products in PWR-MOX spent fuels and computational evaluation using JENDL, ENDF/B, JEF and JEFF. J Nucl Sci Technol. 2008;45:390-401.

[15] Sasahara A. private communication;2013.

[16] Katakura J. A set of ORIGEN2 cross section libraries based on JENDL-3.3 library: ORLIBJ33. Japan: Japan Atomic Energy Agency;2004.

[17] Chiba G. Consistent adjustment of radioactive decay and fission yields data with measurement data of decay heat and β-delayed neutron emissions. Ann Nucl Energy. (submitted).

[18] Chiba G, Narabayashi T. Advanced Bondarenko method for resonance self-shielding calculations in deterministic reactor physics code system CBZ. Ann Nucl Energy. 2016;96;277-286.

[19] Kawamoto Y, Chiba G, Tsuji M, Narabayashi T. Numerical solution of matrix exponential in burn-up equation using mini-max polynomial approximation. Ann Nucl Energy. 2015;80:219-224.

[20] Katakura J. JENDL FP decay data file 2011 and fission yields data file 2011. Japan: Japan Atomic Energy Agency;2011.

[21] Shibata K, Iwamoto O, Nakagawa T, Iwamoto N, Ichihara A, Kunieda S, Chiba S, Furutaka K, Otuka N, Ohsawa T, Murata T, Matsunobu H, Zukeran A, Kamada S, Katakura J. JENDL-4.0: a new library for nuclear science and engineering. J Nucl Sci Technol. 2011;48:1-30.

[22] Koning AJ, Rochman D, Marck S, Kopecky J, Sublet JC, Pomp S, Sjostrand H, Forrest R, Bauge E, Henriksson H, Cabellos O, Goriely S, Leppanen J, Leeb H, Plompen A, Mills R. TENDL-2014: TALYS-based evaluated nuclear data library. URL:`www.talys.eu/tendl-2014.html`;2014

[23] Hagura N, Yoshida T. Analysis of prediction accuracy for actinide decay heat of spent MOX fuel from light water reactors. J At Energy Soc Jpn. 2010;9:29-39. [in Japanese].

Table 1 Employed experimental data for nuclear data adjustment.

Name	Material	Measured form
Fission pulse decay heat (LOWELL)	U-235 element	Beta decay radiation Gamma decay radiation
	Pu-239 element	Beta decay radiation Gamma decay radiation
Fission pulse decay heat (ORNL)	U-235 element	Beta decay radiation Gamma decay radiation
	Pu-239 element	Beta decay radiation Gamma decay radiation
	Pu-241 element	Beta decay radiation Gamma decay radiation
Fission pulse decay heat (YAYOI)	U-238 element	Beta decay radiation Gamma decay radiation
PIE data	UO_2 fuel	38 FP & 17 actinide
	MOX fuel	40 FP & 1 actinide

Table 2 Employed covariance data of nuclear data.

Name	Nuclide	Form	Library
Capture cross section	Actinide	Covariance	JENDL-4.0
Capture cross section	FP	Covariance	TENDL-2014
Fission cross section	Actinide	Covariance	JENDL-4.0
(n,2n) cross section	Actinide	Covariance	JENDL-4.0
(n,2n) cross section	FP	Covariance	TENDL-2014
Fission yield	FP	Covariance	JENDL/FPY-2011
Half life	FP	Standard deviation	JENDL/FPD-2011
Decay energy	FP	Standard deviation	JENDL/FPD-2011
Decay branching ratio	FP	Standard deviation	JENDL/FPD-2011

Figure Captions

Figure 1 Uncertainty curve of target decay heat in short-term cooling period ($0.1\sim10^5$ [s]).

Figure 2 Uncertainty curve of target decay heat in long-term cooling period ($0.1\sim10^3$ [yr]).

Figure 3 Relative differences of calculation values to experimental ones (C/E-1), measurement uncertainty and nuclear data induced uncertainty.

Figure 4 Relative differences of calculation values to experimental ones (C/E-1), measurement uncertainty and nuclear data induced uncertainty in UO_2 case.

Figure 5 Relative differences of calculation values to experimental ones (C/E-1), measurement uncertainty and nuclear data induced uncertainty in MOX case.

Figure 6 Correlation matrices between target decay heat uncertainty in short-term cooling period and uranium-235 fission pulse decay heat uncertainty.

Figure 7 Correlation matrices between target decay heat uncertainty in long-term cooling period and uranium-235 fission pulse decay heat uncertainty.

Figure 8 Correlation matrices between target decay heat uncertainty in short-term cooling period and PIE isotopic concentration uncertainty. The nuclides are the same as Figures 4and 5.

Figure 9 Correlation matrices between target decay heat uncertainty in long-term cooling period and PIE isotopic concentration uncertainty. The nuclides are the same as Figures 4and 5.

Figure 10 Target decay heat uncertainty curves which are before and after adjustment using fission pulse experimental data.

Figure 11 Target decay heat uncertainty curves which are before and after adjustment using PIE data.

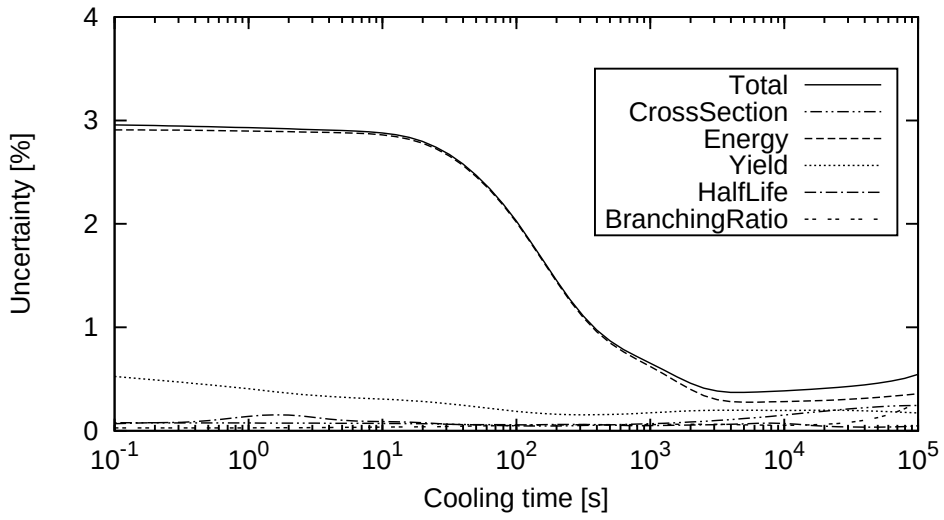


Figure 1 Uncertainty curve of target decay heat in short-term cooling period ($0.1 \sim 10^5$ [s]).

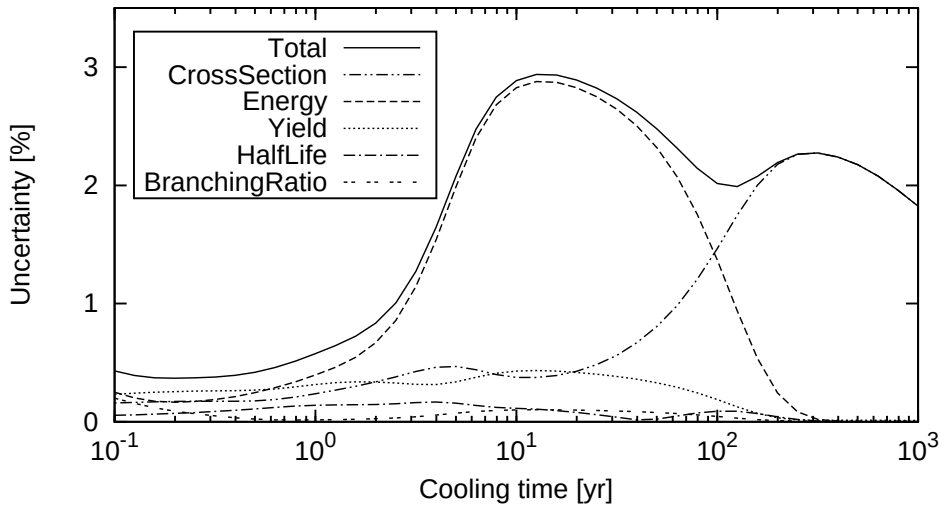
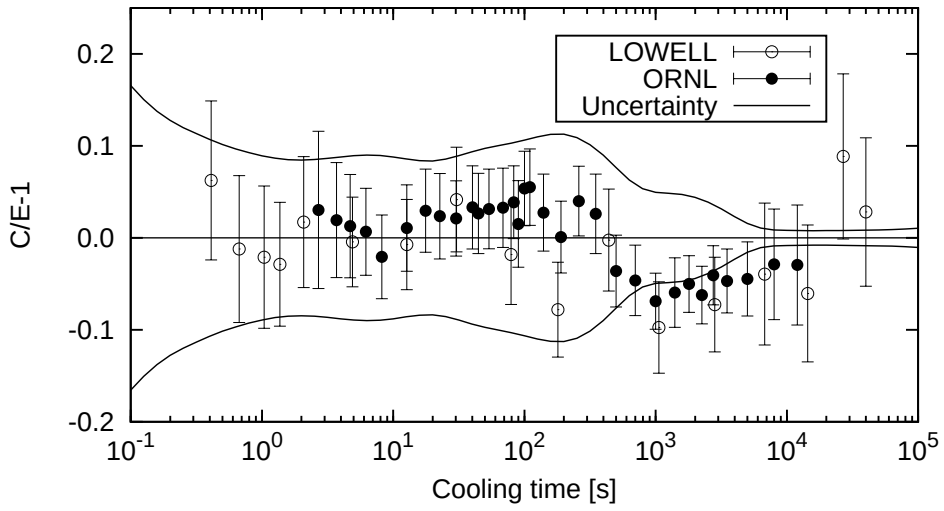
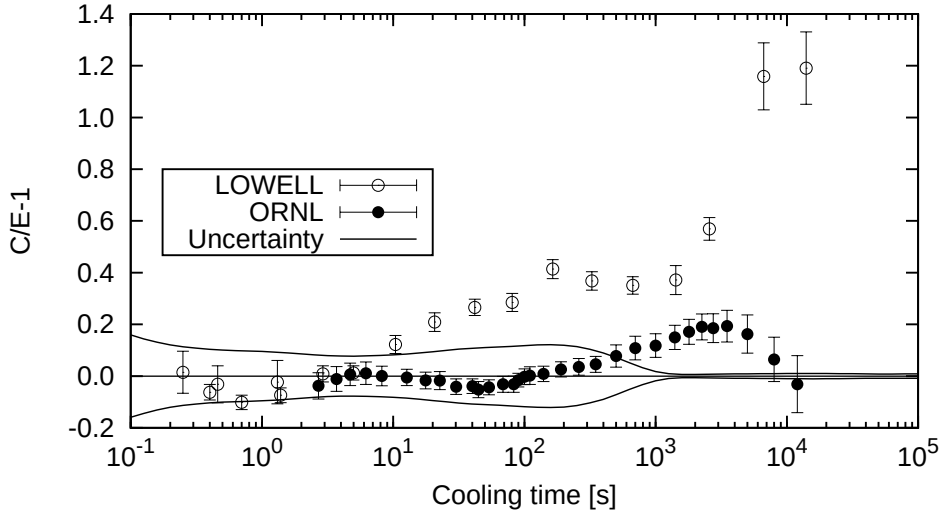


Figure 2 Uncertainty curve of target decay heat in long-term cooling period ($0.1\sim10^3$ [yr]).

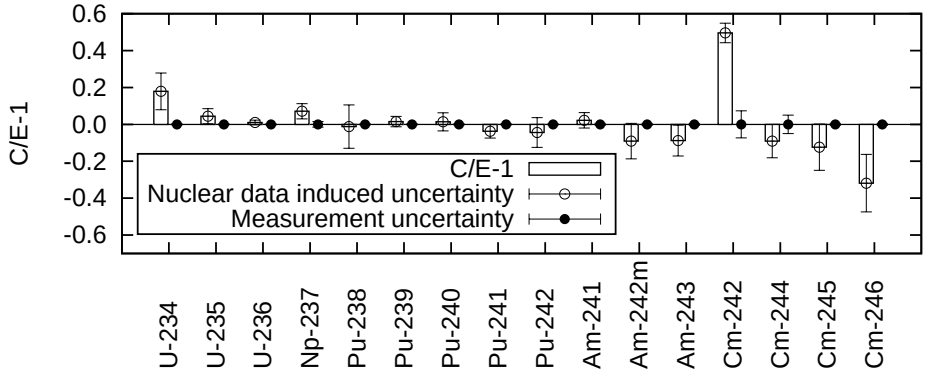


(a) β radiation

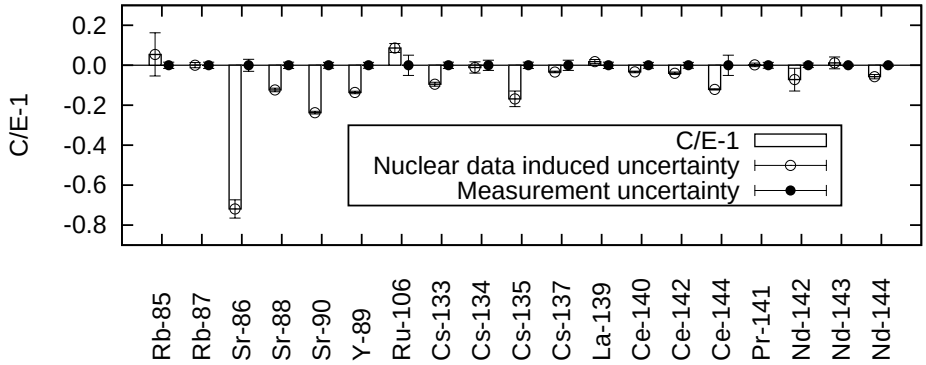


(b) γ radiation

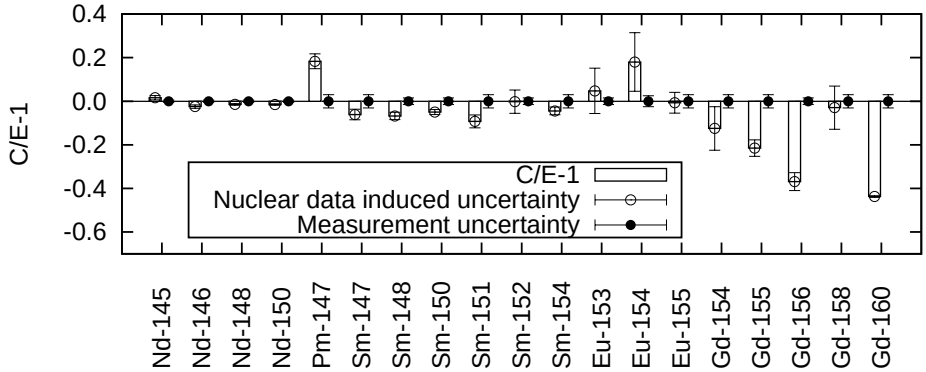
Figure 3 Relative differences of calculation values to experimental ones (C/E-1), measurement uncertainty and nuclear data induced uncertainty.



(a) Actinide

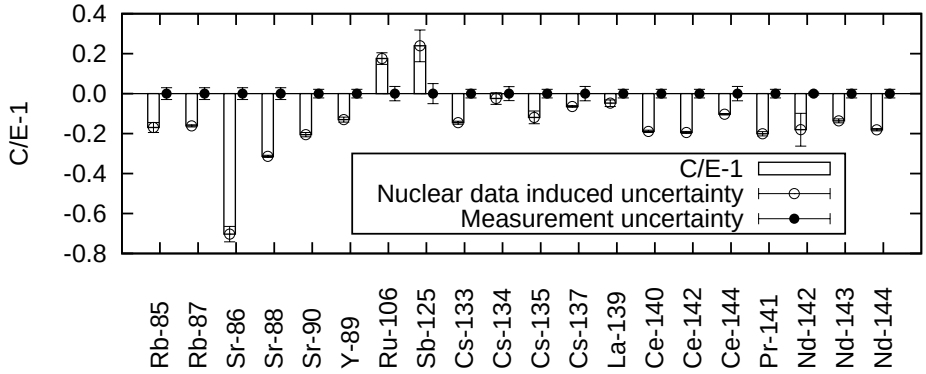


(b) Fission product (1)

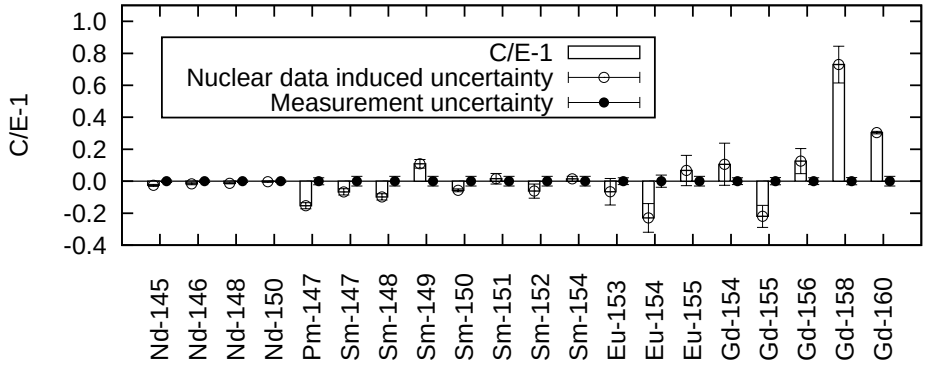


(c) Fission product (2)

Figure 4 Relative differences of calculation values to experimental ones (C/E-1), measurement uncertainty and nuclear data induced uncertainty in UO_2 case.

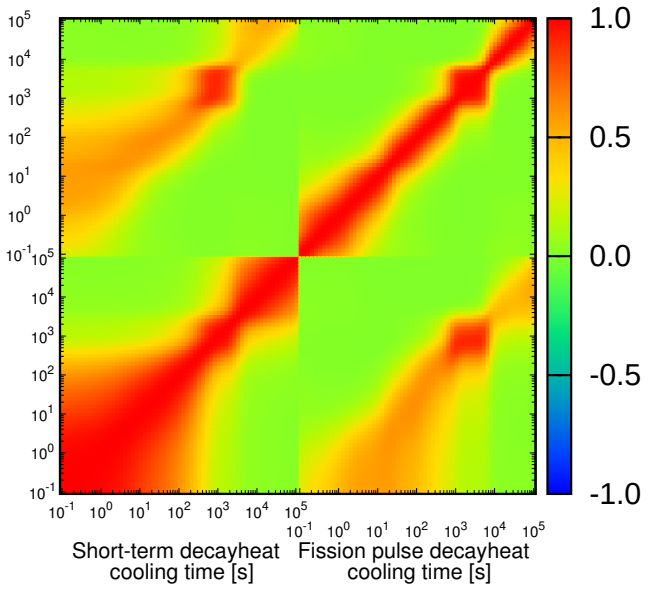


(a) Fission product (1)

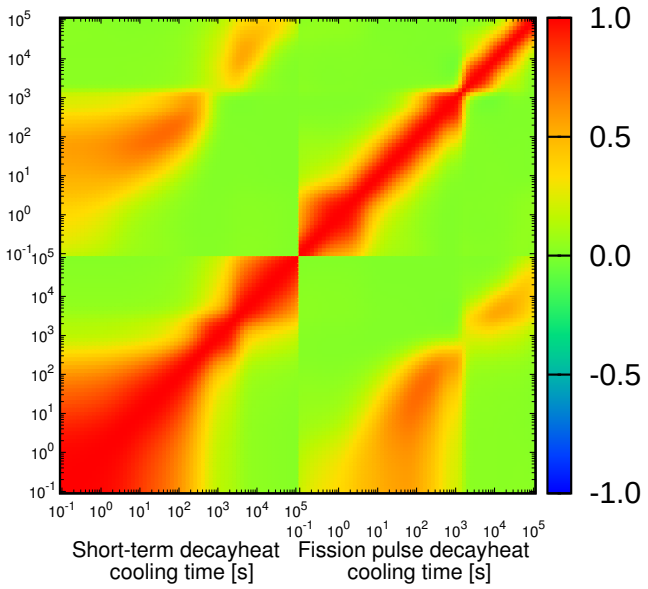


(b) Fission product (2)

Figure 5 Relative differences of calculation values to experimental ones (C/E-1), measurement uncertainty and nuclear data induced uncertainty in MOX case.

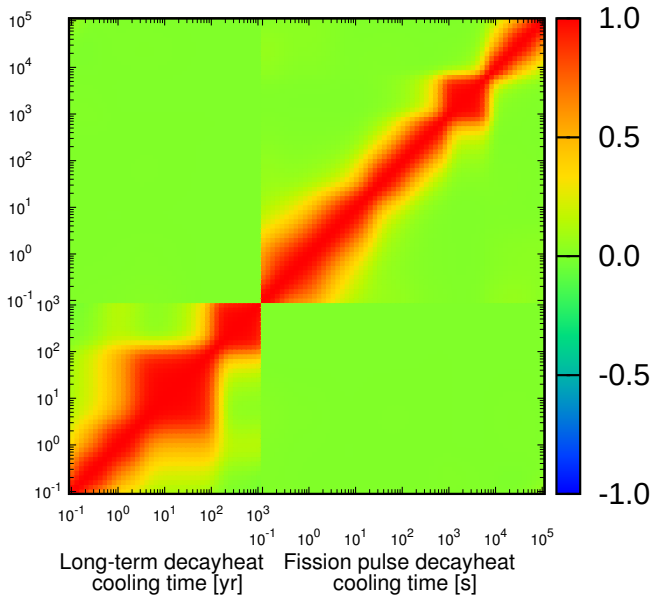


(a) Short-term decay heat v.s. fission pulse decay heat (β radiation)

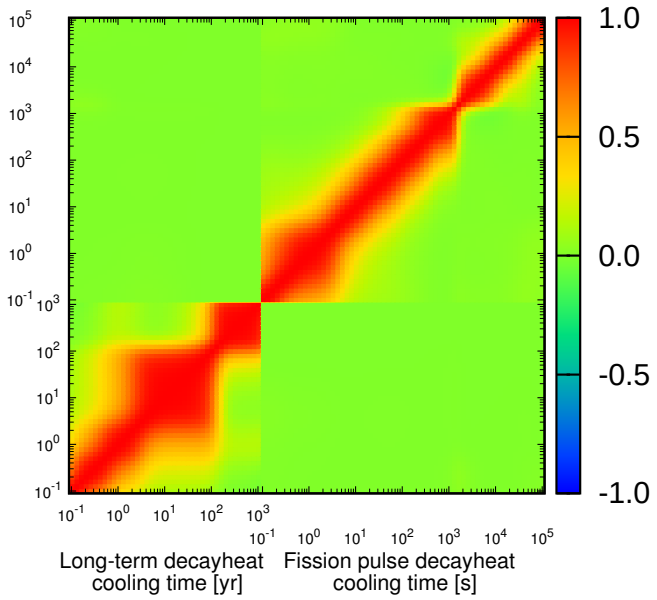


(b) Short-term decay heat v.s. fission pulse decay heat (γ radiation)

Figure 6 Correlation matrices between target decay heat uncertainty in short-term cooling period and uranium-235 fission pulse decay heat uncertainty.

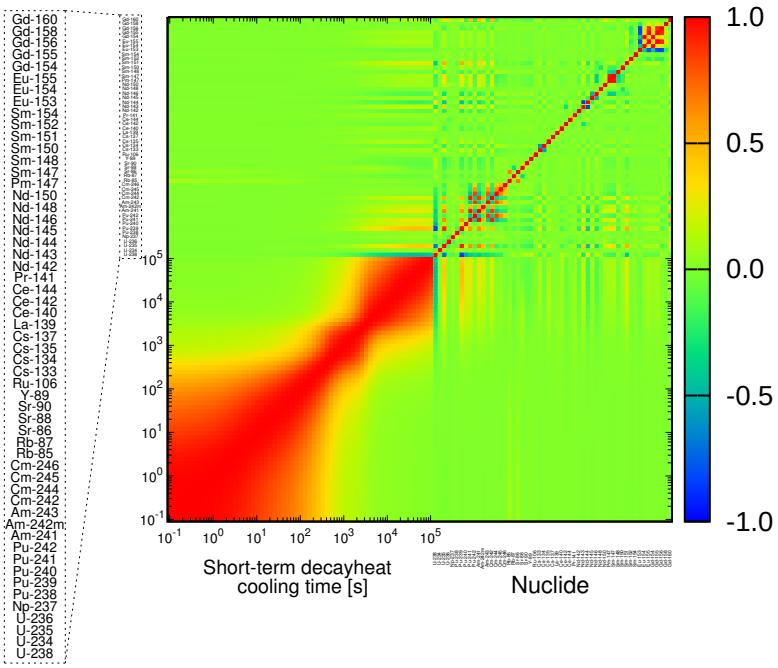


(a) Long-term decay heat v.s. fission pulse decay heat (β radiation)

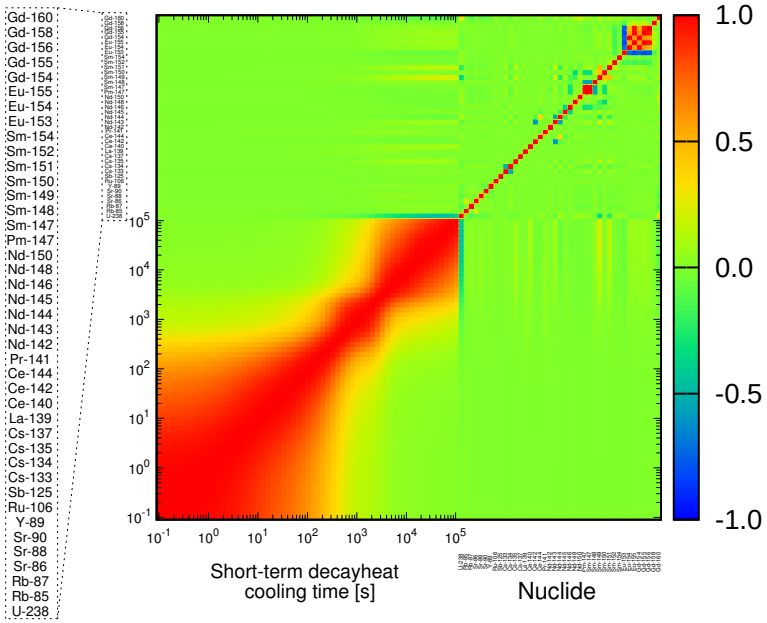


(b) Long-term decay heat v.s. fission pulse decay heat (γ radiation)

Figure 7 Correlation matrices between target decay heat uncertainty in long-term cooling period and uranium-235 fission pulse decay heat uncertainty.

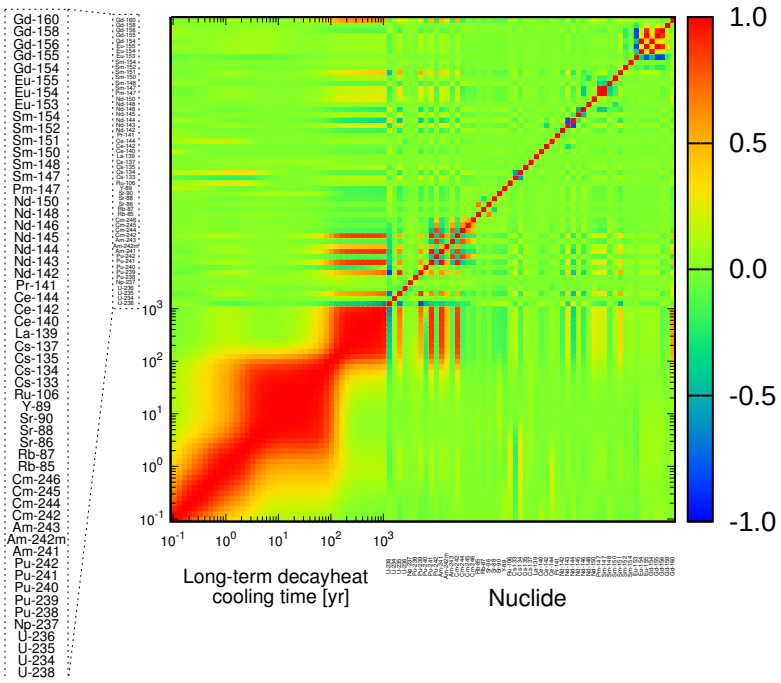


(a) Short-term decay heat v.s. UO_2 fuel PIE data

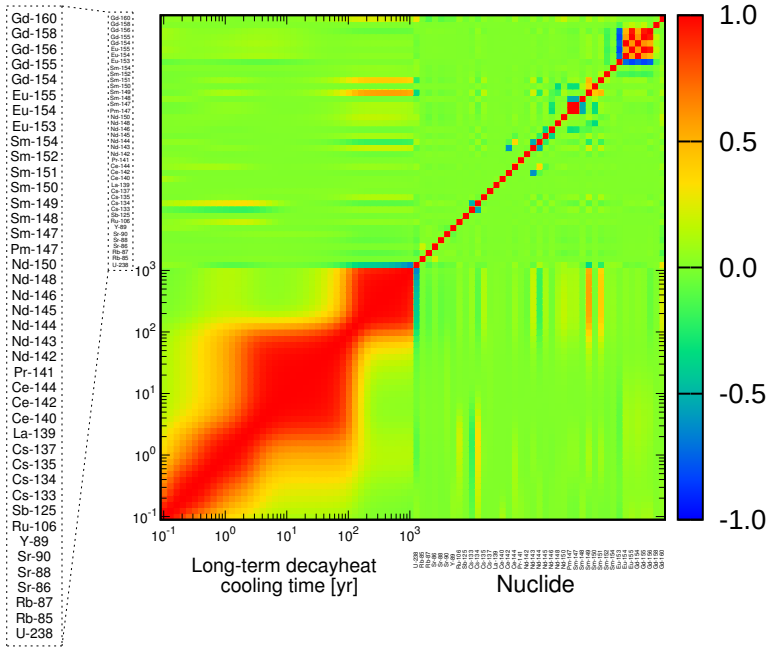


(b) Short-term decay heat v.s. MOX fuel PIE data

Figure 8 Correlation matrices between target decay heat uncertainty in short-term cooling period and PIE isotopic concentration uncertainty. The nuclides are the same as Figures 4 and 5.

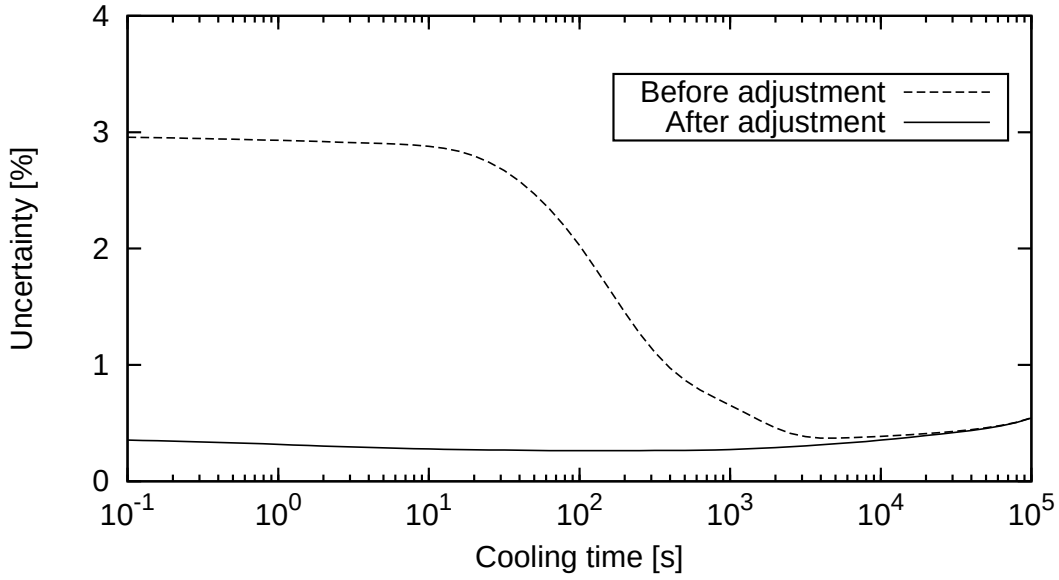


(a) Long-term decay heat v.s. UO_2 fuel PIE data

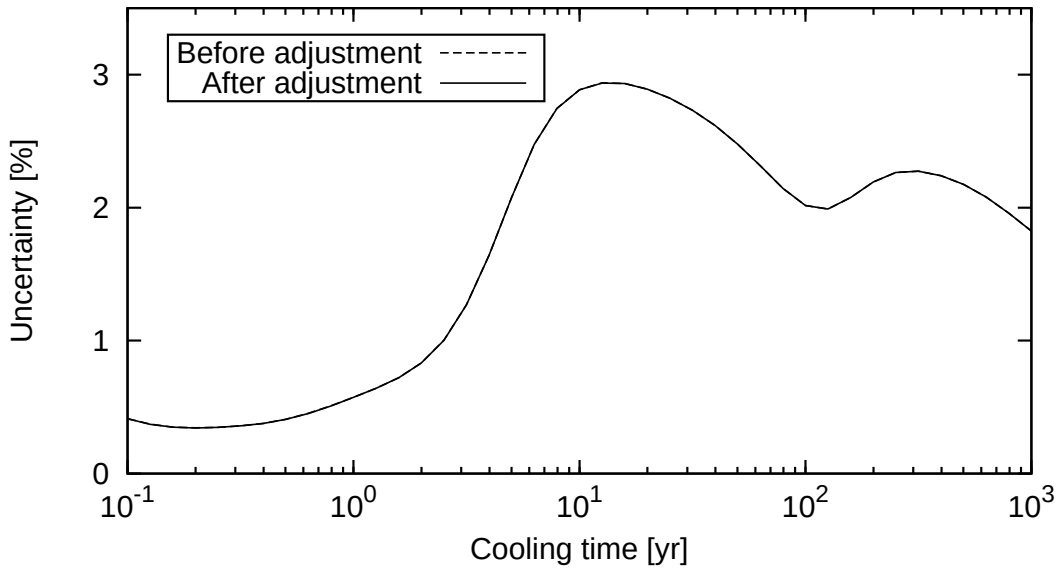


(b) Long-term decay heat v.s. MOX fuel PIE data

Figure 9 Correlation matrices between target decay heat uncertainty in long-term cooling period and PIE isotopic concentration uncertainty. The nuclides are the same as Figures 4 and 5.

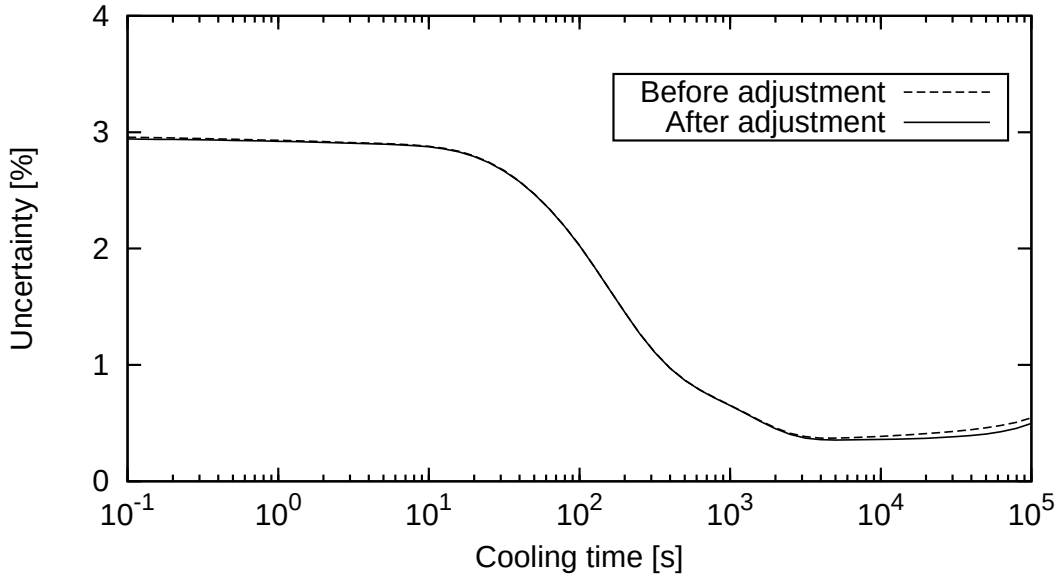


(a) Short-term decay heat

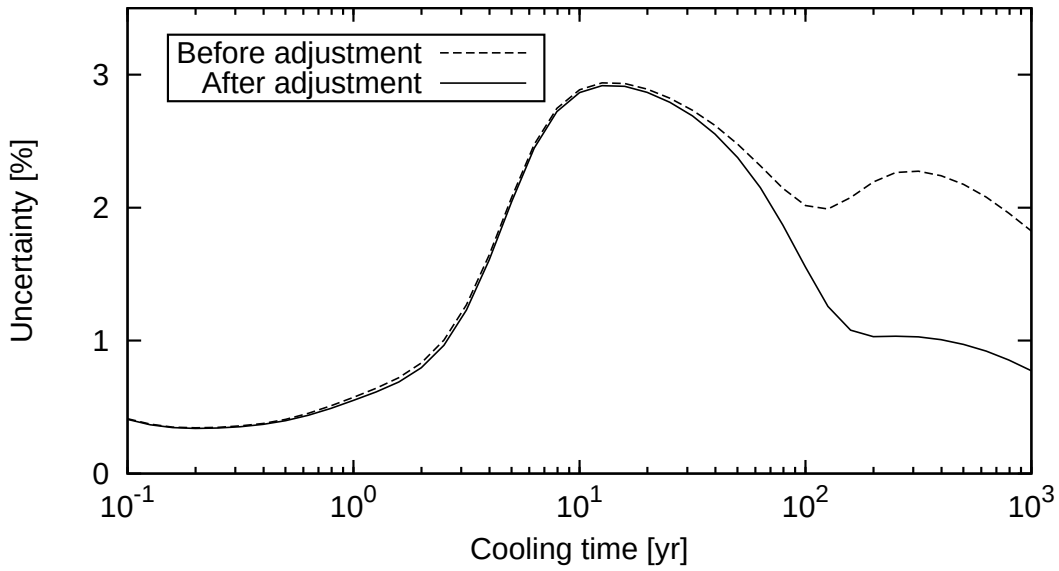


(b) Long-term decay heat

Figure 10 Target decay heat uncertainty curves which are before and after adjustment using fission pulse experimental data.



(a) Short-term decay heat



(b) Long-term decay heat

Figure 11 Target decay heat uncertainty curves which are before and after adjustment using PIE data.